A Hidden Markov, Multivariate Autoregressive (HMM-mAR) Network Framework for Analysis of Surface EMG (sEMG) Data

Joyce Chiang, Z. Jane Wang, *Member, IEEE*, and Martin J. McKeown

***Abstract*—As the primary noninvasive means to assess muscle activation, the surface electromyogram (sEMG) is of central importance for the study of motor behavior in both clinical and biomedical applications. However, multivariate sEMG analysis is complicated by the fact that data recorded during dynamic contractions are inherently nonstationary. To model this nonstationarity and to determine the dynamic muscle activity patterns during reaching movements, we propose combining hidden Markov models (HMMs) and multivariate autoregressive (mAR) models into a joint HMM-mAR framework. We further propose constructing muscle networks statistically by performing a second level, group analysis on the subject-specific models. Network structural features are subsequently investigated as input features for the purpose of classification. The proposed approach was applied to real sEMG recordings collected from healthy and stroke subjects during reaching movements. When examining group muscle networks, we note that specific muscle connection patterns were selectively recruited during reaching movements and were differentially recruited after stroke compared to healthy subjects. As the analysis was performed on the raw data, the amplitude and the underlying "carrier data" of sEMG signals, we notice that the HMM-mAR model fits the amplitude data well, but not the raw or carrier data. The proposed sEMG analysis framework represents a fundamental departure from existing methods where only the amplitude is typically analyzed or the mAR coefficients are directly used for classification. As the method may provide additional insights into motor control, it appears a promising approach warranting further study.**

***Index Terms*—Classification tree, expectation maximization (EM) algorithm, hidden Markov model (HMM), multivariate autoregressive (mAR) model, stroke, surface electromyography (sEMG).**

I. Introduction

THE SURFACE ELECTROMYOGRAPHIC (sEMG) signal is a semistochastic signal whose properties depend upon a number of factors including the anatomical and physiological properties of the contracting muscle, the amount of subcutaneous fat, and choice of electrodes [1]. Since sEMG reflects underlying muscle activity and allows researchers to noninvasively record several muscles simultaneously, it has been widely investigated in the area of motor behavior.

A topic of increasing interest in motor control is to determine how different muscles efficiently collaborate or interact together during natural movements. Though traditionally sEMG recordings are widely examined in a univariate fashion, recent studies suggest that sEMGs recorded from spatially distributed muscles are correlated with each other [2]. Consistent with long-standing clinical observations, this has led to the concept of synergies [3], that is, coordinated activation of groups of muscles. It is suggested that the central nervous system (CNS) may integrate synergies, as opposed to individual muscles, to coordinate muscle activity patterns.

In the past few years, several different methods have been applied to noisy sEMG data to infer synergistic actions and revealed meaningful interactions between muscles, such as principal component analysis (PCA), linear independent component analysis (ICA) [2], [4], and nonnegative matrix factorization (NMF) [5]. These partially linear decomposition methods operate on a common assumption of a smaller numbers of common sources, meaning that a small set of source signals are upstream of the muscles and produce the sEMG signals. They are characterized by a number of latent variables, and thus the multivariate sEMG data can be represented by subspace projections. For example, ICA assumes that the observations are combinations of statistically independent components, and its objective is to find underlying sources. Here, we explore a different approach, multivariate autoregressive mAR modeling, to directly represent interactions between muscles without using latent variables. Methods such as P/ICA do not explicitly reveal interactions but implicitly through underlying sources. Also, models such as P/ICA are instantaneous models, excluding temporal information and quantifying only instantaneous dependencies. However, interactions between muscles may not be instantaneous. The mAR process, widely applied for modeling the temporal dynamics of multivariate systems, can characterize interregional dependencies within multiple channels in terms of the historical influence one variable has on another. As we are working on sEMG multivariate time series, we propose investigating mAR model to deal with the temporal lag between muscles. Thus the synergies extracted impart complementary knowledge, as they include the temporal aspects of muscle coordination compared to the instantaneous methods like P/ICA.

Another common assumption implied in models such as P/ICA is that the muscle activity patterns are time-invariant

Manuscript received April 19, 2007; revised March 8, 2008. The associate editor coordinating the review of this manuscript and approving it for publication was Dr. Yonina C. Eldar.

J. Chiang and Z. J. Wang are with the Department of Electrical and Computer Engineering, University of British Columbia, Vancouver, BC V6T 1Z4, Canada (e-mail: joycehc@interchange.ubc.ca; zjanew@ece.ubc.ca).

M. J. McKeown is with the Pacific Parkinson's Research Centre, University of British Columbia, Vancouver, BC V6T 2B5, Canada (e-mail: mmckeown@interchange.ubc.ca).

Digital Object Identifier 10.1109/TSP.2008.925246

throughout the movements investigated. However, significant time-dependent correlations can be shown to exist between muscle channels during most natural movements, suggesting a complex interplay and coordination between muscles in time-varying fashion. It is widely accepted that the sEMG signals recorded from natural behaviors, such as reaching, as opposed to isometric contractions, are nonstationary. Clinically, reaching movements are considered to consist of an initial phase, under "open loop" control, where feedback is less critical, and a "closed loop" control phase, where feedback is important [6]. In particular, in people with diseases of the cerebellar hemispheres, initial portions of reaching movements are smooth, but an intention tremor becomes prominent towards the end of movements. The time-varying and nonstationary properties implied by open-loop and closed-loop phases of reaching suggests that techniques assuming stationarity (e.g. coherence, linear component analysis) may result in misleading interpretations. To address these concerns, a common quasi-static approach is to incorporate a sliding time window into the original signal models, such that the stationarity assumption is valid in a piecewise sense. However, the selection of an appropriate (possibly time-varying) window length is a nontrivial task, and it can have a significant effect on the analysis results [7].

Based on the aforementioned observations, in this paper we propose combining hidden Markov models (HMMs) and multivariate autoregressive mAR models into an HMM-mAR framework for modeling nonstationary multivariate sEMG time series and determining dynamic muscle activity patterns during reaching movements. HMM-mAR is advantageous for modeling sEMG data for a number of reasons. First, an mAR model allows full representation of multivariate sEMG signals, so it naturally captures the dependency relationships between different channels. The results can be explored further to reveal muscle associations and synergies. Furthermore, given that the data are nonstationary and we have no prior knowledge on when the mAR models may change, incorporating HMM provides a probabilistically tractable and robust way of modeling the dynamic changes of state (i.e., different mAR models) [8]. HMM-mAR, also known as AR model with Markov regime, has been widely used in econometrics, target tracking, and statistical signal processing [9], but has not been commonly applied to biophysiological data. Cassidy and Brown [10] applied HMM-mAR to electrophysiological signals for the purpose of spectral estimation. In the present paper, we extend prior approaches to investigate the suitability of HMM-mAR for sEMG signals and study dynamic interactions among muscles during reaching.

In addition, we also explore different forms of sEMG data for further analysis. A sEMG signal can be considered as a zero-mean, band-limited, and wide-sense stationary stochastic process (referred to as "carrier data" here) modulated by the EMG amplitude [11], and it has been suggested that carrier data can be approximately modeled as a Gaussian process. As it is assumed that the amplitude data represent muscle activity from numerous individual muscle fibers, a common, traditional practice in the EMG literature is to focus on the amplitude of the sEMG signal, which can be obtained by rectifying and low-pass filtering the raw sEMG signal, in effect discarding the carrier data. Recently, an increasing number of studies have been reported working on raw, unrectified sEMG signals. For instance, linear ICA was applied to noisy raw sEMG data and revealed meaningful interactions between muscles [4]. In [12], a multivariate autoregressive (mAR) model was explored to model multichannel raw sEMG signals. To the best of our knowledge, no previous studies have focused on the carrier data of sEMG signals, yet our very recent study suggests that the carrier data may also be informative [13]. In this paper, to have a better understanding of sEMG and its nature, we will use a fundamentally different approach and model different forms of the sEMG signals: raw sEMG, amplitude data and carrier data.

In real biomedical applications, it is commonly required to extrapolate results from few subjects to an entire population in order to explore, for example, changes in reaching movements after stroke. The analysis requires methods to meaningfully integrate results from individual subjects and rigorously compare the results across groups. To address this intersubject variability issue, we employ statistical analysis to investigate consistent muscle collaboration patterns across subjects within a given subject group.

The main contributions of this paper are as follows:

- Presents an HMM-mAR framework for modeling the muscle activities during reaching movements using sEMG signals;
- Constructs muscle networks and suggests that structural features appear robust to intersubject variability; and
- Investigates the results of model-fitting when the proposed analysis is performed on raw, amplitude and carrier data of sEMG signals.

The paper is organized as follows. In Section II, we describe the proposed HMM-mAR framework and discuss different forms of sEMG signals. A classification scheme is proposed for classifying sEMG signals collected from healthy and stroke subjects. The classification results are discussed in Section III.

II. Methods

In this section, we first describe the HMM-mAR framework, whose state parameters, including mAR coefficients, are estimated using the expectation maximization (EM) algorithm. We then introduce the amplitude-modulated model of sEMG signal. Finally, we describe the process of constructing muscle networks and propose a classification scheme based on the learned HMM-mAR model. For the remainder of the paper, we use bold letters to represent vectors and matrices.

A. HMM-mAR Model

We propose modeling the multichannel sEMG data using a hidden Markov-model multivariate autoregressive (HMM-mAR) process. An HMM-mAR model can be considered as a variant of a regular mAR model. The key difference is that in HMM-mAR, the model parameters, including mAR coefficients and noise covariance, are no longer time-invariant, but are modulated by an unobserved Markov chain. In other words, the HMM-mAR model switches between different "submodels," each of which has its own set of parameters, and thus the resulting time series is piecewise stationary. A good

introduction to a first-order HMM-mAR model can be found in [14], where it is referred to as a switching AR model. In our paper, we consider a more general HMM-mAR model of order P.

For simplicity, we assume that the hidden Markov chain is discrete, first order, and the mAR model is of order P. The multivariate sEMG data is formulated as

$$\boldsymbol{y}_k + \sum_{p=1}^{P} \boldsymbol{a}_p(s_k)\boldsymbol{y}_{k-p} = \boldsymbol{w}_k(s_k), \quad 1 \le k \le T \tag{1}$$

where T denotes the total number of time points. $\boldsymbol{y}_k \in \mathbb{R}^M$ denotes the observed M-channel sEMG signal at time k, and in this paper, $M = 7$. s_k is the hidden Markov chain at time k, and it can be in one of the distinct states $\{1, 2, \ldots, Ns\}$. The state transition of the Markov chain is governed by the following two parameters: (i) transition probability matrix $\boldsymbol{A} \in \mathbb{R}^{Ns \times Ns}$, with elements $A_{ij} = Pr(s_{k+1} = j | s_k = i)$, and (ii) initial state probability $\boldsymbol{\pi} \in \mathbb{R}^{Ns}$, where $\pi_i = Pr(s_1 = i)$. $\boldsymbol{a}_p(s_k = i) \in \mathbb{R}^{Ns \times Ns}$ is the mAR coefficient matrix at time lag p given that s_k is in state i. The noise term $\boldsymbol{w}_k(s_k = i) \sim N(0, \boldsymbol{\Sigma}_i) \in \mathbb{R}^M$ is assumed to be an M-dimensional Gaussian with zero mean, and its covariance matrix $\boldsymbol{\Sigma}_i$ is determined by the hidden state s_k. In summary, the complete parameter set of the HMM-mAR process can be specified as follows:

$$\lambda = (\boldsymbol{A}, \pi, \boldsymbol{a}_p(i), \boldsymbol{\Sigma}_i), \quad 1 \le i \le Ns. \tag{2}$$

B. Parameter Estimation via EM Algorithm

Given that only $\boldsymbol{Y}_{1:T} = (\boldsymbol{y}_1, \boldsymbol{y}_2, \ldots, \boldsymbol{y}_T)$ is observed and state transition of s is unknown, we use the expectation maximization (EM) algorithm to obtain the maximum likelihood (ML) estimate of the model parameters. A good introduction to the EM algorithm can be found in [15]. The key steps of the EM algorithm are (1) *Expectation step (E-step)* which computes the expectation of the likelihood function by including unobserved data as if they were observed, and (2) *Maximization step (M-step)* which updates the estimate of model parameters by maximizing the expected likelihood function computed in E-step. The EM algorithm keeps alternating between E-step and M-step until convergence is reached in a ML sense. Dey *et al.* [9] has shown the derivation of the EM algorithm for univariate HMM-AR models. We extended their work and derived the EM algorithm for the HMM-mAR model. Since the derivation for the HMM-mAR model is similar to the classic HMM model, here we only list the key results as follows:

E-step: This step evaluates the auxiliary likelihood function, $Q(\cdot)$. To facilitate the description of the auxiliary likelihood function, we first introduce two new variables, $\alpha_k(i)$ and $\beta_k(i)$. The forward variable $\alpha_k(i)$ is defined as $\alpha_k(i) = Pr(\boldsymbol{Y}_{1:k}, s_k = i | \lambda)$, and the backward variable $\beta_k(i)$ is $\beta_k(i) = Pr(\boldsymbol{Y}_{k+1:T} | s_k = i, \lambda)$. They can be recursively computed via the well-known forward-backward procedure as follows:

$$\alpha_{k+1}(j) = \sum_{i=1}^{Ns} \alpha_k(i) A_{ij} b_j(\boldsymbol{y}_{k+1}) \quad k = 1, 2, \ldots, T-1 \quad \text{and} \quad 1 \le j \le Ns \tag{3}$$

$$\beta_k(i) = \sum_{j=1}^{Ns} A_{ij} b_j(\boldsymbol{y}_{k+1}) \beta_{k+1}(j) \quad k = T-1, T-2, \ldots, 1 \quad \text{and} \quad 1 \le i \le Ns \tag{4}$$

where $b_j(\boldsymbol{y}_k)$ denotes the observation symbol probability distribution in state j, and is defined as $b_j(\boldsymbol{y}_k) = Pr(\boldsymbol{y}_k | s_k = j, \boldsymbol{Y}_{k-P:k-1}, \lambda)$. Given that the noise follows a Gaussian distribution, $b_j(\boldsymbol{y}_k)$ can be written as $N(\boldsymbol{y}_k + \sum_{p=1}^{P} \boldsymbol{a}_p(j)\boldsymbol{y}_{k-p} | 0, \boldsymbol{\Sigma}_j)$. The next step is to compute the $Q(\cdot)$ function by taking the expectation of complete data log likelihood as follows:

$$\begin{aligned} Q(\lambda) &= E\left\{ \log Pr(\boldsymbol{Y}_{1:T}, \boldsymbol{s}_{1:T} | \lambda) | \boldsymbol{Y}_{1:T}, \lambda^{old} \right\} \\ &= \sum_{i=1}^{Ns} \gamma_1(i) \log \pi_i + \sum_{k=1}^{T} \sum_{i=1}^{Ns} \sum_{j=1}^{Ns} \xi_k(i,j) \log A_{i,j} \\ &\quad - \frac{1}{2} \sum_{k=1}^{T} \sum_{i=1}^{Ns} \gamma_k(i) \left\{ \log |\boldsymbol{\Sigma}_i| + \left[\boldsymbol{y}_k + \sum_{p=1}^{P} \boldsymbol{a}_p(i)\boldsymbol{y}_{k-p} \right]^T \right. \\ &\quad \left. \times \boldsymbol{\Sigma}_i^{-1} \left[\boldsymbol{y}_k + \sum_{p=1}^{P} \boldsymbol{a}_p(i)\boldsymbol{y}_{k-p} \right] \right\} \end{aligned} \tag{5}$$

where

$$\gamma_k(i) \triangleq Pr(s_k = i | \boldsymbol{y}_{1:T}, \lambda) = \frac{\alpha_k(i)\beta_k(i)}{\sum_{j=1}^{Ns} \alpha_k(j)\beta_k(j)} \tag{6}$$

$$\begin{aligned} \xi_k(i,j) &\triangleq Pr(s_k = i, s_{k+1} = j | \boldsymbol{y}_{1:T}, \lambda) \\ &= \frac{\alpha_k(i) A_{ij} b_j(\boldsymbol{y}_{k+1}) \beta_{k+1}(i)}{\sum_{i=1}^{Ns} \sum_{j=1}^{Ns} \alpha_k(i) A_{ij} b_j(\boldsymbol{y}_{k+1}) \beta_{k+1}(i)}. \end{aligned} \tag{7}$$

M-step: This step reestimates the model parameter λ by computing $\arg_\lambda \max Q(\lambda)$ and it yields

$$A_{ij} = \frac{\sum_{k=1}^{T-1} \xi_k(i,j)}{\sum_{k=1}^{T-1} \gamma_k(i)} \tag{8}$$

$$\begin{aligned} \boldsymbol{\Sigma}_i &= \frac{1}{\sum_{k=1}^{T} \gamma_k(i)} \sum_{k=1}^{T} \gamma_k(i) \left[\boldsymbol{y}_k + \sum_{p=1}^{P} \boldsymbol{a}_p(i)\boldsymbol{y}_{k-p} \right] \\ &\quad \times \left[\boldsymbol{y}_k + \sum_{p=1}^{P} \boldsymbol{a}_p(i)\boldsymbol{y}_{k-p} \right]^T \end{aligned} \tag{9}$$

$$\begin{aligned} \boldsymbol{B}(i) &\triangleq (\boldsymbol{a}_1(i)\boldsymbol{a}_2(i) \cdots \boldsymbol{a}_P(i)) \\ &= -\left[\sum_{k=1}^{T} \gamma_k(i) \boldsymbol{y}_k \boldsymbol{z}_{k-1}^T \right] \left[\sum_{k=1}^{T} \gamma_k(i) \boldsymbol{z}_{k-1} \boldsymbol{z}_{k-1}^T \right]^{-1} \end{aligned} \tag{10}$$

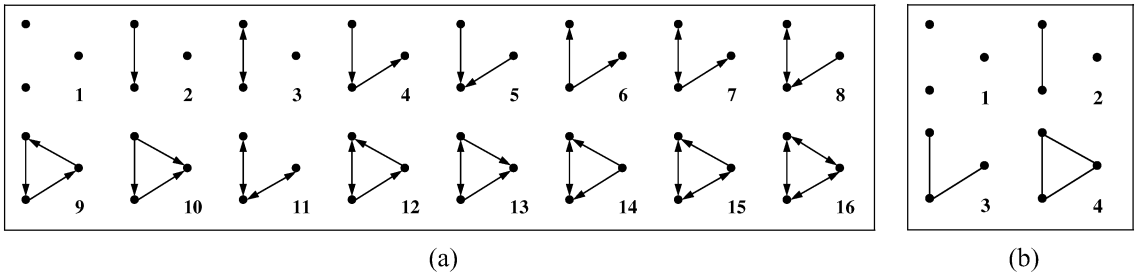

Fig. 1. (a) Labels for directed triple subnetworks. (b) Labels for undirected triple subnetworks.

where

$$\boldsymbol{z}_{k-1} \triangleq (\boldsymbol{y}_{t-1}, \boldsymbol{y}_{t-2}, \cdots, \boldsymbol{y}_{t-P})^T. \tag{11}$$

By maximizing the $Q(\cdot)$ function at each iteration, the likelihood function will increase and eventually converge to a local maximum. Once the maximum likelihood estimates of the model parameters have been obtained, the optimal state sequence $\{s_1, s_2, \ldots, s_T\}$ can be found via the Viterbi algorithm [16].

C. Statistical Analysis for Muscle Network Construction

1) Muscle Networks and 3-Node Subnets: Since mAR coefficients and residual covariance matrix of HMM-mAR models characterize the temporal and spatial correlation between muscle signals, they are exploited to reveal the dynamic association patterns between muscles during natural movements in this paper. Specifically, we employ ideas from graph theory and use directed and undirected graphs to represent the connectivity between muscles observed in mAR coefficients and covariance matrices, respectively. In the graph, each muscle is represented by a node. A directed graph is constructed from mAR coefficient matrices by selecting the top n largest off-diagonal elements of the matrix and drawing directed edges between the corresponding muscle pairs. For instance, if element (i, j) of the matrix is selected, a directed edge is drawn from node j to node i indicating that muscle j is exerting influence on muscle i. Examples of directed graphs constructed from mAR coefficient matrices with $n = 20$ are shown in Fig. 8. An undirected graph can be constructed from a standardized covariance matrix in a similar fashion by forming edges between muscle pairs corresponding to the top n coefficients. Since covariance matrices are symmetric, connections between selected muscle pairs are represented by undirected edges.

A natural movement such as a reaching movement is typically considered to consist of a sequence of submovements. Each individual submovement can involve coactivations of multiple spatially distributed muscles. This observation motivates us to look at subnetworks which comprise a smaller set of muscles nodes in the original muscle connectivity graph. Given a graph with M nodes, C_M^k distinct subnetworks can be extracted, where C denotes binomial coefficient and k is the number of nodes in subnetworks. In this paper, similar to [17], we will focus on subnetworks consisting of three muscle nodes, which we call *triple* subnets. These subgraphs can be succinctly characterized by the connection patterns between muscle nodes. Specifically, a directed triple subgraph derived from an mAR coefficient matrix can have 16 different connection patterns [see Fig. 1(a)], whereas an undirected subgraph derived from a covariance matrix has four different patterns [see Fig. 1(b)]. Based on the connection pattern between muscle nodes, each triple subgraph is assigned a label, and these labels can be further used as classification features for differentiating muscle networks from two different groups. Details are explained in Section II-D.

2) Statistical Analysis: The intra- and intersubject variability is a common and challenging issue in biomedical studies. In particular, two issues need to be addressed here for muscle network construction by using the model parameters. One concerns with intrasubject variability: how to statistically infer a muscle network from a single subject performing multiple repeated trials? The other is about intersubject variability: how to infer muscle network features shared by a group of subjects rather than subject-specific features? Extrapolating results from one trial (or one subject) to an entire group requires methods that can meaningfully integrate results from individual trials and rigorously compare the results across groups. In this paper, we perform a group analysis for each muscle connection in the muscle network through the Analysis of Variance (ANOVA) [18], which tests the effects of multiple factors on the data.

To statistically construct a muscle network for each subject performing repeated trials, for each connection, the estimated mAR coefficients are input to perform a t-test with the null hypothesis that the coefficients come from a distribution with a zero mean. It is should be noted that, to ensure a common distribution of the coefficients under the null hypothesis, the standard deviation of each mAR coefficient estimate is also determined and used to normalize the mAR coefficients from different trials before performing the hypothesis test. The muscle network is then constructed by including all statistically significant connections, that is, connections whose p-values are smaller than a predefined threshold (0.05 in our case). Similarly, the group muscle network from different subjects within the same group can be constructed. Examples are shown in Fig. 7. To identify group differences, each mAR coefficient is analyzed using one-way ANOVA with a group factor (e.g., healthy group vs. stroke group). The identified significant connections are plotted together as a network to illustrate the group difference [see Fig. 8(c) and Fig. 9(c)].

As an alternative to analyzing the model parameters directly, we also examine the group difference by investigating the structural features extracted from each individual muscle network. In this case, p-value of each connection for each single trial is calculated by t-test. By comparing the p-values of all connections to a predefined threshold (e.g., 0.05), we can represent the structural features of the muscle network by a binary vector of length N, with N being the total number of connections. To identify significant group differences, the binary vectors from two different groups (e.g., health group and stroke group) are input to perform a two-sided Wilcoxon rank sum test. The returned p-value for each tested connection are subsequently compared to a predefined threshold to identify significantly different connections statistically. For comparison with the results from analyzing the coefficient parameters directly, examples are shown in Fig. 8(d) and Fig. 9(d).

D. Feature Extraction and Classification

1) Structural Feature Extraction: To classify between stroke and healthy subjects based on the estimated parameters of the HMM-mAR models, one possible approach is to extract structural features from the muscle connectivity graphs derived from mAR coefficient and/or covariance matrices. Two types of structural features are considered: *edges* and *triples*. The *edge* feature is essentially a string of 1's and 0's, each of which denotes the presence of a connectivity between a given muscle pair (1 for connected pair and 0 for disconnected pair). To obtain *edge* features, we first convert the connectivity graph of m nodes into an adjacency matrix, T, where element $t_{ij} = 1$ if there is an edge going from node j to node i and $t_{ij} = 0$ otherwise. Since the connectivity graphs were constructed to be loop-free, the diagonal elements of T are all zeros and are neglected for the classification purpose. The off-diagonal elements of the adjacency matrix are then concatenated to form a binary vector of $M(M-1)$ elements, and this is referred to as *edge* feature. The other structural feature is based on the triple subgraphs extracted from the muscle connectivity graphs (see Section II-C). For an M-node connectivity graph, C_M^3 triple subgraphs can be extracted, and each subgraph is assigned a label according to its connection pattern, as described in the previous section. For classification purpose, the labels of all C_M^3 subgraphs are put together to form a categorical feature vector or *triple* feature vector.

2) Classification: To classify the structural features extracted from the muscle connectivity graphs, we chose classification trees as classifiers in this paper. Classification trees were chosen over other classifiers, such as support vector machine (SVM), since they are more suitable for categorical data [19]. Furthermore, tree-based classifiers are known for their ability in selecting features which produce largest separation of objects from different classes. Therefore, the classification results can help us identify the muscle recruitment patterns which best differentiate between stroke and healthy subjects. On the other hand, because SVM implicitly map feature vectors into a high dimensional space, the results are harder to interpret.

The performance of cross-subject classifications is evaluated using a leave-one-subject-out cross-validation scheme, where each time, all N trials of a subject are held out to serve as test samples while the remaining trials of other subjects are used to train the classifier. The class label of the test subject is determined by the majority vote of the classified test trials.

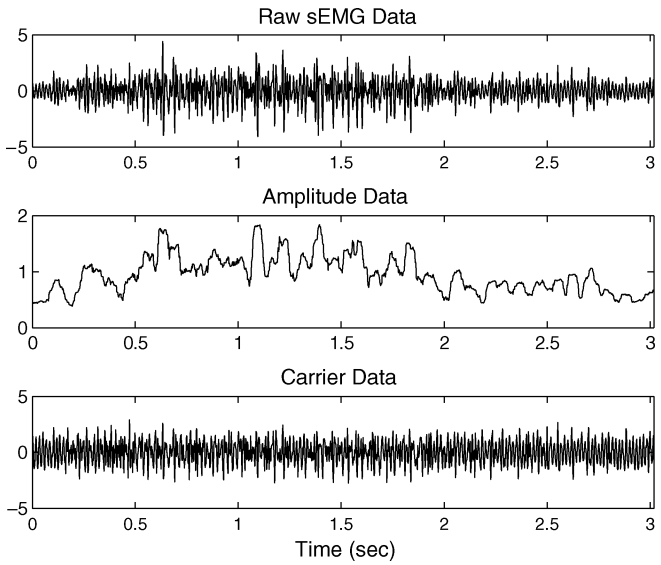

Fig. 2. Three forms of sEMG signal: raw sEMG data, amplitude data, and carrier data.

E. Comparative Classification Scheme Proposed by Hu and Nenov

In addition to structural features, there are alternative ways of extracting features from the learned mAR model. In Hu and Nenov's work [12], they proposed constructing feature vectors directly from mAR coefficient matrices by concatenating all the entries in the matrix into a vector of PM^2 elements, where P denotes the order of the mAR model and M denotes the number of muscles being looked at. A maximal likelihood classifier was employed to classify these feature vectors. In our paper, we adopted a similar approach. First, we concatenated all entries of a mAR coefficient matrix to form a M^2-element feature vector, assuming that the mAR model is of order 1. Because of the high dimension of the feature space, we used PCA for dimension reduction. The new feature vectors composed of principal component coefficients were classified using SVM [20]. This classification scheme will later be compared with the one based on structural features.

F. Amplitude-Modulated sEMG Representation

Clancy *et al.* [11] have suggested that a sEMG signal $y(k)$ recorded during voluntary dynamic contractions can be considered as a zero-mean, band-limited, and wide-sense stationary stochastic process $x(k)$ modulated by the EMG amplitude $m(k)$ such that

$$y(k) = x(k)m(k) \tag{12}$$

where k indicates time. To distinguish $x(k)$ from $y(k)$, we refer to $x(k)$ as the "carrier data." In the literature, there have been several techniques proposed for accurate amplitude estimation [11]. One that is used in this paper is root-mean-square (RMS), with a moving window applied. The optimal window length may

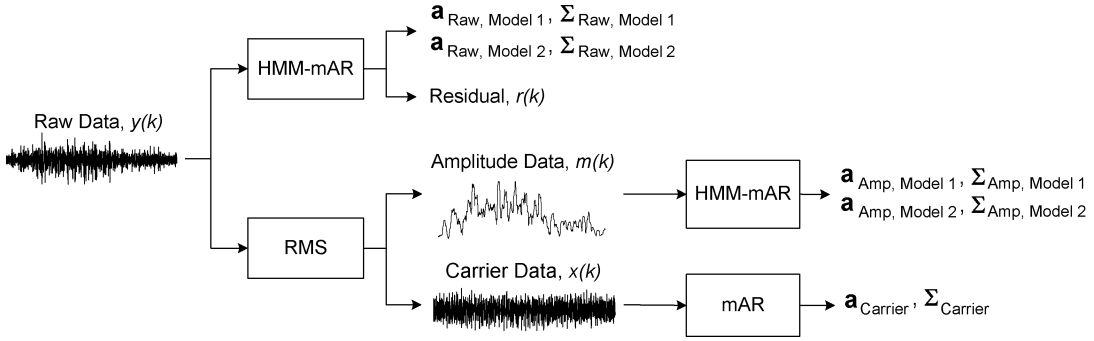

Fig. 3. Flowchart summarizing processing steps performed on various form of sEMG data.

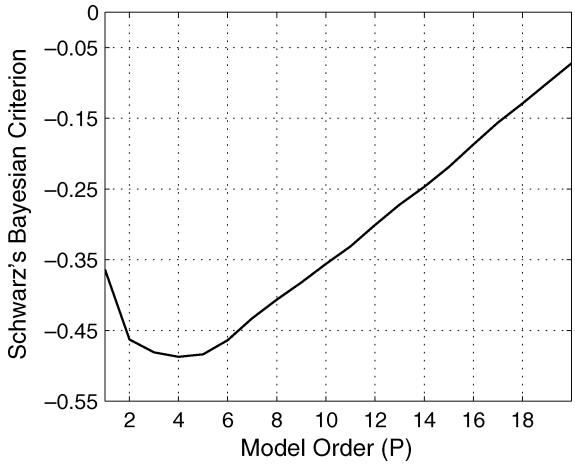

Fig. 4. Model order selection using the Schwarz's Bayesian Criterion. The optimal order is the one which gives the lowest SBC, and it is around $P = 4$ in this case.

be estimated by the sampling frequency and tasks performed [11]. For this paper, we used RMS with a window length of 50 ms, or equivalently, 30 data points at the sampling frequency of 600 Hz. Based on the estimated amplitude $m(k)$, the carrier stochastic process $x(k)$ can be calculated by dividing the raw sEMG signal $y(k)$ by the estimated amplitude $m(k)$. Fig. 2 shows a segment of raw sEMG data and the estimated amplitude and carrier components. The resulting carrier data, $x(k)$, can be approximately represented as a zero-mean Gaussian process [11] and is wide-sense stationary. Thus, it can be modeled by a regular mAR model.

To our knowledge, almost all existing sEMG analysis techniques focus on amplitude data, and the carrier is simply ignored, but our very recent work suggests that the carrier can also be informative and may provide additional insights into the underlying reaching movements [21]. Therefore, in this paper, we propose applying HMM-mAR/mAR framework to the following three forms of sEMG data: the raw data $y(k)$, the amplitude data $m(k)$, and the carrier data $x(k)$. The processing steps are summarized in the flowchart shown in Fig. 3.

G. sEMG Data Collection and Preprocessing

Nine healthy and nine stroke subjects were recruited from the community to perform reaching tasks. During the experiment, each subject was first seated in a chair with their hands on the thigh and was instructed to reach and touch a fixed target after hearing an auditory cue. The target was located in the subject's mid-sagittal plane at shoulder height, and its distance with the subject was adjusted such that it is just within the workspace of the paretic arm of stroke subject or nondominant arm of healthy subject. For every subject, the reaching task was performed five times on paretic side of stroke subjects and nondominant side of healthy subjects, resulting in 90 trials in total. The relevant clinical data of the stroke subjects, including motor impairment as assessed by the Fugl-Meyer scale, injury location, and hand dominance, were detailed in [22].

The electrical activities of seven muscles (the anterior and lateral deltoid, long head and lateral head triceps, biceps brachium, latissimus dorsi, and the brachioradialis) were recorded using surface electrodes (self-adhesive, silver, silver-chloride pellet electrodes with 7 mm diameter, fixed interelectrode distance of 30 mm). The 7-channel sEMG signals were amplified, sampled at 600 Hz, and high-pass filtered at 20 Hz to reduce movement-related artifact. More details on the sEMG experimental procedures can be found in [22].

Since a number of factors could influence the amplitude of the sEMG (e.g., exact positioning of the electrodes, movement of the muscle with respect the electrodes, the amount of subcutaneous fat, and the impedance of the skin) and may not necessarily be task-related, to minimize trial-to-trial variability, we first normalize the raw sEMG signals to zero mean and unit variance. After normalizing the sEMG signals, we denoised the sEMG data using the empirical mode decomposition (EMD) technique [23]. The applicability of the EMD method to sEMG data analysis has been demonstrated by our prior work [24]. EMD decomposes a univariate time series into a sum of intrinsic mode functions (IMF). For the purpose of this paper, we used the sum of the first three IMF's of each channel in place of the original sEMG data.

III. A Case Study

In this section, we evaluate the performance of the proposed HMM-mAR framework for modeling the sEMG data and discuss the classification results when applied to data collected from stroke and healthy subjects.

A. Fitting of HMM-mAR

First, we study the dynamic changes of state during reaching movements by fitting an HMM-mAR model to the raw multi-

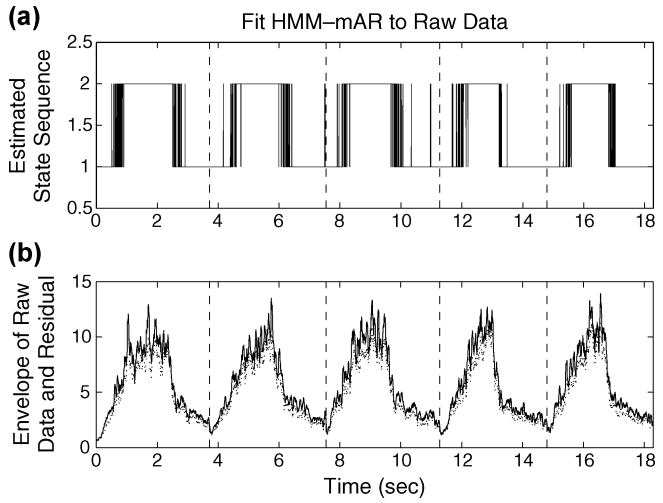

Fig. 5. Fitting a fourth-order HMM-mAR model to raw sEMG data obtained from a stroke subject over five consecutive reaching trials. The top panel (a) shows the estimated state sequence of a 2-state hidden Markov chain. The bottom panel (b) shows the envelopes of the raw sEMG data (solid line) and the residual of the fitted HMM-mAR model (dotted line).

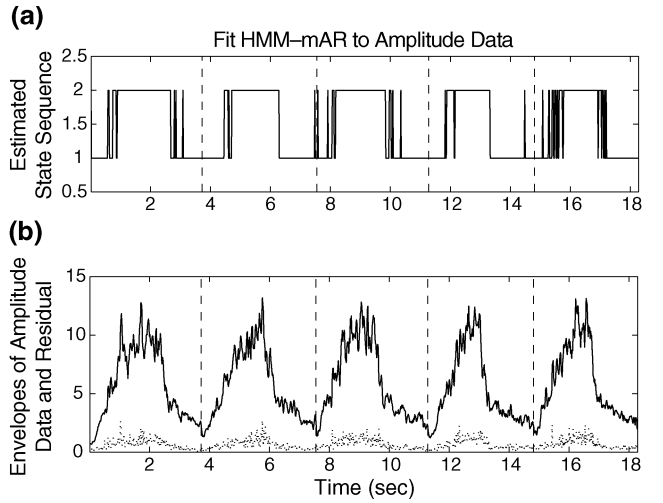

Fig. 6. Fitting a fourth-order HMM-mAR model to the amplitude component of sEMG data from the same stroke subject as in Fig. 5. The top panel (a) shows the estimated state sequence which is more stable than the case of raw data as shown in Fig. 5. Moreover, the estimation performance has greatly improved as indicated by the significant reduction in the magnitude of the residual (dotted line in the bottom panel).

channel sEMG signals. The order of the model is determined by Schwarz's Bayesian Criterion (SBC), which is shown by Lütkepohl [25] to yield the smallest mean-squared prediction error for fitted AR models. In our case, a fourth-order HMM-mAR model is chosen based on SBC (see Fig. 4) to fit to the raw sEMG data. An example of the estimated state sequence obtained from a stroke subject over five reaching trials is shown in Fig. 5(a). It can be seen that the proposed approach segmented each reaching movement into two sections: the initial phase (State 1), and the full-movement phase (State 2). This pattern is relatively consistent across five trials as shown in Fig. 5, suggesting that the proposed technique is robust enough to segment data regardless of the different onset latencies in individual muscles. Also, it is encouraging to note that the states of the Markov chain remain relatively stable in each phase despite the fluctuation in the amplitudes of the sEMG signals.

When we looked closely at the residuals after HMM-mAR fitting, we noticed that regardless of the AR model order P, HMM-mAR provides very poor prediction performance when applied to the raw sEMG signals,where large residuals were observed [Fig. 5(b)]. Based on this observation, we believe that the residuals may also be informative and should not be naively ignored. In Section III-C, we will show that the structural features extracted from covariance matrices of the residuals actually yield good classification performance.

Further, we applied the proposed approach to the amplitude data. An example is shown in Fig. 6, where a fourth-order model was chosen based on SBC. It is clear that the residuals are sufficiently small, indicating that sEMG amplitude data are well modeled by the HMM-mAR approach. We also examined the carrier data. Since the carrier data are shown to be wide-sense stationary, instead of using an HMM-mAR model, we fitted a regular mAR model to the carrier data. The results are similar to those observed from raw sEMG data in the sense that both signals are both poorly predicted by the models and, therefore, large residuals are observed. Our later classification results from

TABLE I
THE RATIO OF RMS VALUES OF RESIDUALS TO RMS OF sEMG SIGNALS FOR DIFFERENT FORMS OF sEMG

	Raw Data	Amplitude Data	Carrier Data
Ratio	84.37%	13.64%	83.95%

using the carrier data show that, similar to the residuals, the carrier can be informative too, despite the fact that it is ignored by traditional analysis approaches.

B. Analysis of Muscle Networks

As aforementioned in Section II-C, both mAR coefficient and covariance matrices of the fitted HMM-mAR or regular mAR can be used to construct muscle connectivity networks. For illustration purposes, here we focus on using the first-order model.

We first examine the results of muscle networks statistically constructed for each subject. As an example, the muscle networks corresponding to State 2 of the estimated state sequence in Fig. 5(a) are illustrated in Fig. 7. Fig. 7(a) shows statistically significant $(p < 0.05)$ mAR coefficients estimated from a single reaching trial whereas Fig. 7(b) shows significant mAR coefficients across all five trials as determined by t-test. In spite of the trial-to-trial variability in the raw sEMG data [see Fig. 5(b)], the muscle networks are relatively consistent across trials, indicating the robustness of the proposed scheme to intrasubject variability.

We further analyze the group muscle networks of healthy and stroke subjects. Examples of group networks constructed using raw and carrier data are shown in Fig. 8 and Fig. 9, respectively. Fig. 8(c) and Fig. 9(c) show significantly different $(p < 0.05)$ connections between healthy and stroke groups based on mAR coefficients, where as Fig. 8(d) Fig. 9(d) show connections based on structural features.

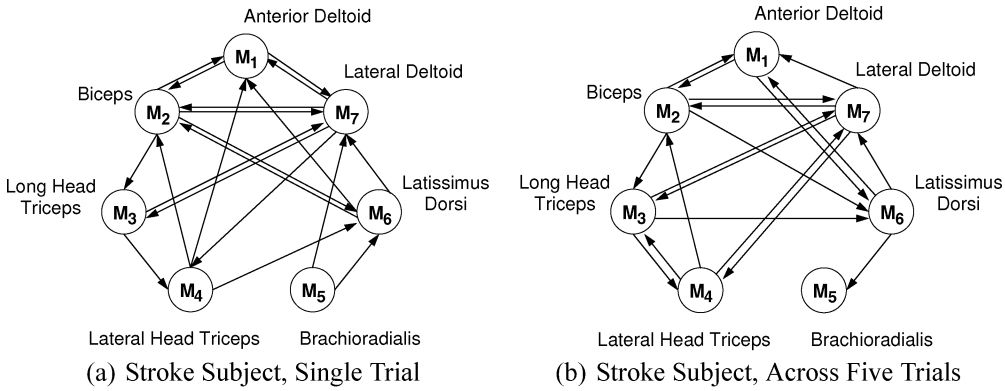

Fig. 7. Muscle networks of a stroke subject extracted from Model 2 mAR coefficients using the same data as in Fig. 5. The edges correspond to statistically significant mAR coefficients with p-values below 0.05 as determined by t-test. (a) Muscle network of a single trial. (b) Muscle network with significant connections across all five trials.

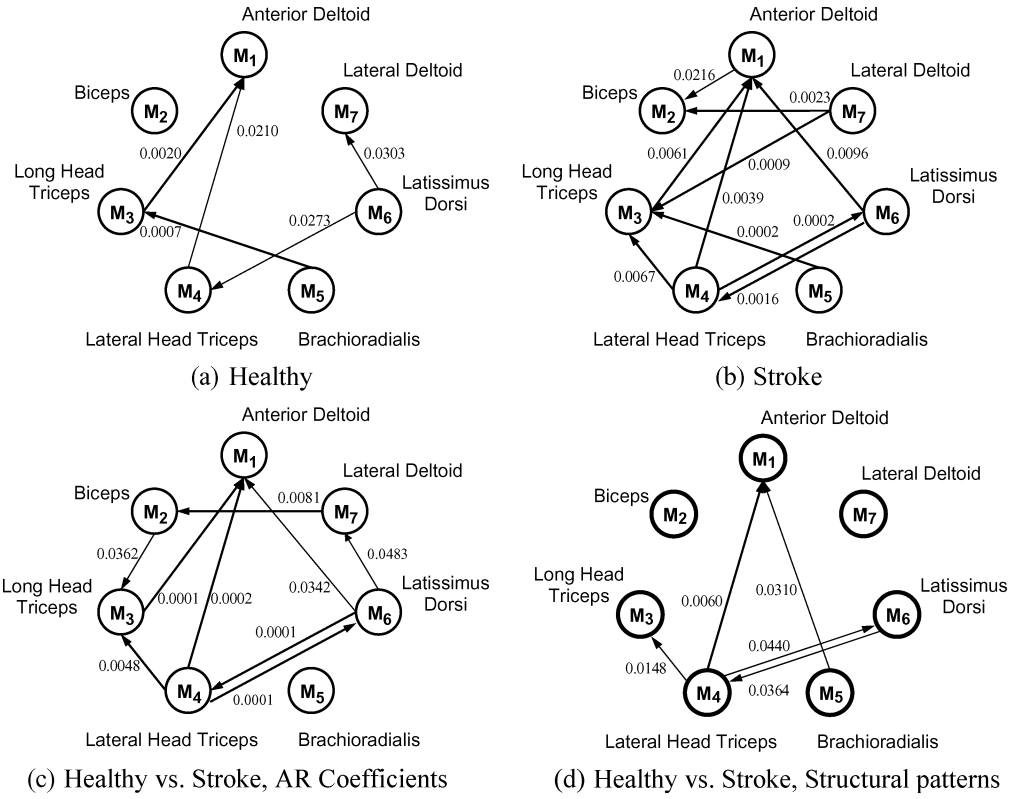

Fig. 8. Group muscle networks statistically extracted from Model 2 mAR coefficient matrices of the HMM-mAR model fitted to raw data. Model 2 corresponds to the full-movement phase. The p-value of each connection is shown beside the edge. Only connections with p-values below 0.05 are shown. (a) Group muscle network of the healthy subjects. (b) Group muscle network of the stroke subjects. (c) Significantly different connections between healthy and stroke subjects, based on mAR coefficients. (d) Significantly different connections between healthy and stroke subjects, based on structural patterns.

It can be seen that in both figures, the healthy and stroke groups share several common connections, suggesting a similarity in the synergistic muscle patterns recruited by two groups. Moreover, stroke subjects have substantially more connections than healthy subjects. In particular, in Fig. 8, Anterior Deltoid and Lateral Deltoid are more highly connected with other muscles in the stroke group than in the healthy group. This result is consistent with the findings reported by Eng *et al.* in [22], where they analyzed the same dataset using traditional univariate techniques and observed that additional muscles, such as Lateral Deltoid and Biceps, were recruited by stroke subjects to compensate the weakness in the Anterior Deltoid during reaching movements. Similar observations are noted in Fig. 9.

The results also exemplify the co-contraction of muscles in stroke subjects. Significant coupling between the Lateral Head of Triceps and Latissimus Dorsi, and Lateral Head of Triceps and Anterior Deltoid are seen in stroke subjects to a greater degree than normal subjects. As these muscle pairs are not directly antagonistic or agonistic, this probably reflects less efficient recruitment strategies after stroke.

TABLE IV
CROSS-SUBJECT CLASSIFICATION ERROR RATES GIVEN BY mAR COEFFICIENTS

Feature Set	Edges			Triples		
	1	2	3	1	2	3
Raw: AR Coef., Model 1	50.00	22.22	16.67	50.00	33.33	33.33
Raw: AR Coef., Model 2	38.89	22.22	5.56	33.33	22.22	22.22
Carrier: AR Coef.	16.67	22.22	11.11	27.78	22.22	16.67

Cross-subject classification error rates (%) given by mAR coefficients with the SVM as the classifier. Here, the classification features were directly composed from elements of mAR coefficient matrices, in contrast with Table II and III where structural features (i.e., *edges* and *triples*) were used.

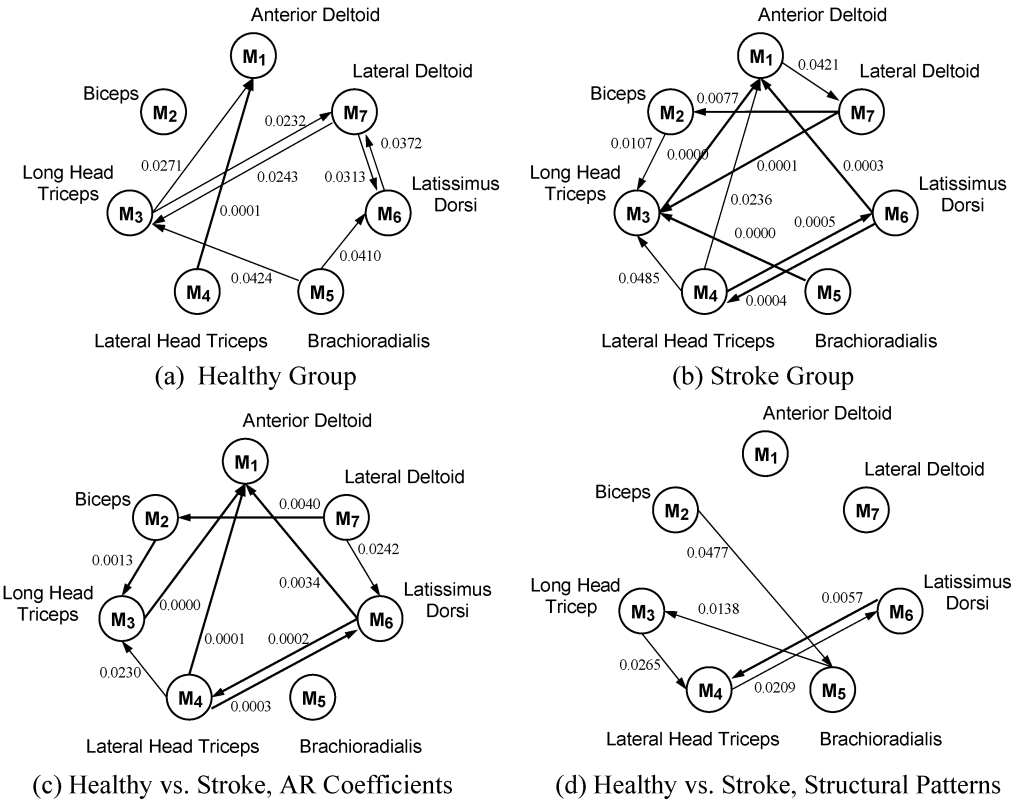

(a) Healthy Group (b) Stroke Group

(c) Healthy vs. Stroke, AR Coefficients (d) Healthy vs. Stroke, Structural Patterns

Fig. 9. Group muscle networks statistically extracted from mAR coefficient matrices of the mAR model fitted to carrier data. The p-value of each connection is shown beside the edge. Only connections with p-values below 0.05 are shown. (a) Group muscle network of the healthy subjects. (b) Group muscle network of the stroke subjects. (c) Significantly different connections between healthy and stroke subjects, based on mAR coefficients. (d) Significantly different connections between healthy and stroke subjects, based on structural patterns.

C. Classification Results

To demonstrate the applicability of the proposed framework, we applied it to data recorded from reaching movements, with the objective of classifying between healthy and stroke subjects. In particular, we focus on comparing the nondominant arm of healthy subjects with the paretic arm of stroke subjects. Although the dominant side of healthy subjects may also be used, the nondominant arm is more comparable to the paretic arm of stroke subjects in terms of their motor capability [22], whereas the dominant arm of healthy individuals is often overtrained for simple tasks such as reaching.

For classification purposes, a first-order, two-state HMM-mAR model is fitted to the raw sEMG data, and a first order mAR model is fitted to the carrier data. In our proposed scheme, classification is performed on structural features, i.e., *edges* or *triples*, extracted from mAR coefficient and residual covariance matrices of the fitted models as described in Section II-D. We let the classification tree do an exhaustive search over all possible subsets of structural features and select the ones which give the lowest error rate. To avoid overfitting, we limit both classification trees and SVMs to use at most three elements of the input features. Based on the model parameters from which structural features are derived, six different sets of features are explored. Table II summarizes the best error rates produced by the classification tree classifiers, where each row represents one set of feature choices. The Table I shows the

TABLE II
CROSS-SUBJECT CLASSIFICATION ERROR RATES GIVEN BY STRUCTURAL FEATURE SETS

Structural Feature Set	Edges			Triples		
	1	2	3	1	2	3
Raw: AR Coef., Model 1	22.22	16.67	11.11	27.78	16.67	11.11
Raw: Residual Cov., Model 1	33.33	22.22	11.11	27.78	11.11	11.11
Raw: AR Coef., Model 2	22.22	16.67	11.11	27.78	27.78	16.67
Raw: Residual Cov., Model 2	27.78	16.67	11.11	27.78	16.67	5.56
Carrier: AR Coef.	27.78	22.22	5.56	27.78	16.67	11.11
Carrier: Residual Cov.	16.67	11.11	11.11	11.11	11.11	5.56

Cross-subject classification error rates (%) given by structural feature sets. Classification trees are used as the classifier. Columns indicate the type and number of features used in classification, whereas the rows indicate the model parameters from which the features are extracted. *Raw* and *carrier* represent the form of sEMG signals to which the HMM-mAR/mAR model is fitted. *AR coef.* and *Residual Cov.* denote the model parameters, mAR coefficient matrix and residual covariance matrix, respectively. *Model 1* corresponds to State 1 of hidden Markov chain, and *Model 2* is State 2. Note that for every mAR coefficient matrix, we used its top 20 largest elements $(n = 20)$ to construct the muscle network, whereas for the residual covariance matrix, the top 12 elements were used.

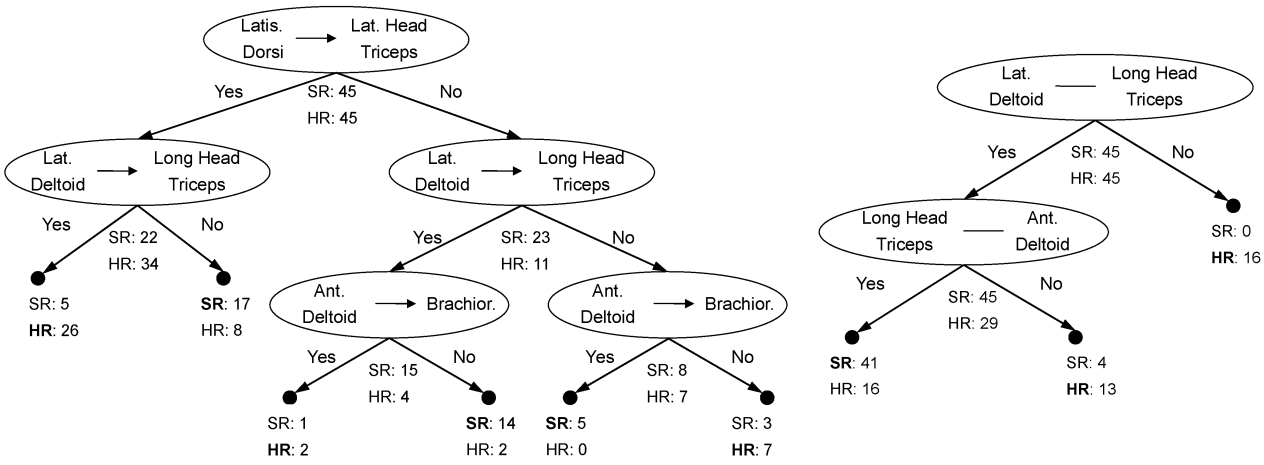

(a) Carrier: AR Coef. (b) Carrier: Residual Cov.

Fig. 10. The best classification trees with *edges* as classification features. (a) Classification tree based on mAR coefficient matrix of mAR model fitted to carrier data. Top 20 elements of the matrix were selected to construct the muscle connectivity network. (b) Classification tree based on residual covariance matrix of mAR model fitted to carrier data. Top 12 elements of the matrix were selected.

ratio of RMS values of residuals after model fitting to RMS of sEMG signals for different forms of sEMG. In summary, we observe that the HMM-mAR model can provide very accurate prediction of the amplitude of the sEMG signals, but yield very large residuals when applied to the raw and the carrier sEMG signals. It suggests that HMM-mAR, and, thus, mAR, could be reasonably good for modeling the amplitude of sEMG signals, but may not be suitable for the raw and carrier signals. corresponding classification trees are shown in Figs. 10 and 11. In these illustrations, Model 1 refers to the estimated model parameters associated with State 1 of the hidden Markov chain, and Model 2 corresponds to State 2. In the rest of the paper, Model 1/2 and State 1/2 are used interchangeably.

In general, the classification error rates drop as we increase the number of features used in classification from 1 to 3. Three features are sufficient for providing excellent classification results (e.g., 10% error rate). When considering the raw data, we noticed that the classification performances from using residual covariance matrices are comparable, if not better, to using mAR coefficient matrices of either Model 1 or Model 2. This observation suggests that the residuals are useful in differentiating different subject groups (i.e., the healthy group and the stroke group in our study). It leads us to believe that the residual is also informative and thus should not be simply ignored as noise. When we compare the classification performance from using Model 1 with that of Model 2, we note that they both produce

TABLE III
CROSS-SUBJECT CLASSIFICATION ERROR RATES GIVEN BY COMBINED STRUCTURAL FEATURE SETS

Structural Feature Set	Edges			Triples		
	1	2	3	1	2	3
Raw: AR Coef., Model 1 + Model 2	22.22	5.56	5.56	27.78	16.67	5.56
Raw: Residual Cov., Model 1 + Model 2	27.78	16.67	11.11	27.78	11.11	5.56

Classification features were derived from mAR coefficient/residual covariance matrices by combining Model 1 and Model 2 extracted from raw sEMG signals.

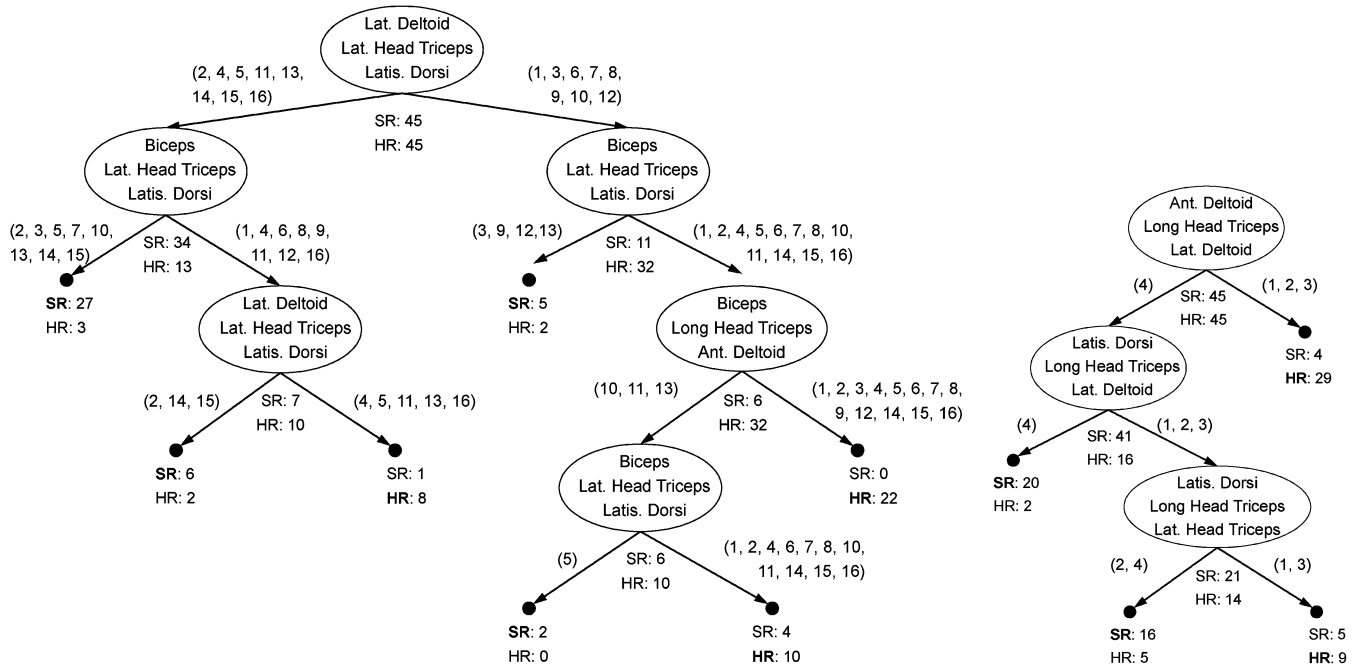

(a) Raw: AR coef., Model 1 (b) Carrier: Residual Cover

Fig. 11. The best classification trees with *triples* as classification features. (a) Classification tree based on mAR coefficient matrix of State-1 HMM-mAR model fitted to raw data. Top 20 elements of the matrix were selected. (b) Classification tree based on residual covariance matrix of mAR model fitted to carrier data. Top 12 elements of the matrix were selected.

good, comparable performances. Since Model 1 and Model 2 represent different portions of the reaching movement, these two representations should provide different but complementary insights into the underlying reaching movements. Such intuition motivates us to combine these structural features from Model 1 and Model 2. As shown in Table III, the performance given by either mAR coefficient matrices or covariance matrices is noticeably better than any individual model.

When comparing the results from using the carrier and the raw sEMG signals, we note that the classification performance of carrier data is comparable to that of raw data. This suggests that the carrier could be informative in characterizing reaching movements.

To evaluate the performance of the proposed classification scheme, we compare it with other mAR-based methods. The first one is similar to the one proposed by Hu *et al.* [12] and it was outlined in Section II-D. In this method, the input features are directly obtained from mAR coefficient matrices by concatenating all elements in the matrices into an input vector. These features are then projected to a lower dimension using PCA before being fed to the SVM classifier. This method gives very poor classification performance, and the average error rate is around 0.5. To have a more fair comparison with the proposed structure-based method, we modified Hu's approach such that the number of features used for classification are also limited to a maximum of three. The results are reported in Table IV. It can be seen that the proposed method significantly outperforms the modified version of Hu's method. The key difference between these two approaches, in terms of feature selection, is that Hu's approach directly uses mAR coefficients as features, whereas the proposed approach uses structural features of the connection patterns between muscle nodes. The results shown in Table II and Table IV imply that the structural features are more robust and less sensitive to intersubject variability than the mAR coefficient values themselves.

IV. CONCLUSION

We have proposed an HMM-mAR framework for sEMG data analysis. Several important issues have been addressed in this framework: the nonstationarity of sEMG signals, group

analysis for intersubject variability, identification of significant muscle connections, statistically-based construction of group muscle networks, and classification across subjects. The proposed framework is able to effectively segment multivariate sEMG series and statistically identify the dynamic muscle association patterns over time. The inferred state sequence of the hidden Markov chain suggests that the underlying motor system may be switching between different muscle recruitment patterns. Similar observations of state switching in limb motor tasks have also been reported in other studies [6], [26]. However, the exact correspondence between the state transition of a Markov chain and the switching in the biological system is yet to be investigated. A reasonable extension of this work would be to use the proposed HMM-mAR framework to first automatically segment the data, and then investigate other methods, such as nonnegative factorization (NNF) [26] for the different segments.

Our sEMG results demonstrate that the proposed HMM-mAR model fits the amplitude signals well. When the framework is applied to raw or carrier data, the resulting residuals are still informative, enabling adequate classification, and should be further investigated.

Our sEMG analysis presents a fundamental departure from most existing methods and suggests that the properties of the sEMG carrier data or the residuals after model fitting are essential for fully characterizing reaching movements. Future work will focus on intersubject variability in muscle association patterns during reaching movements using the carrier data and residuals.

ACKNOWLEDGMENT

The authors would like to thank J. Eng, Ph.D., for providing useful data and helpful discussions regarding current sEMG analysis methods.

REFERENCES

[1] R. Merletti, D. Farina, and A. Granata, "Non-invasive assessment of motor unit properties with linear electrode arrays," *Electroencephalogr. Clin. Neurophysiol. Suppl.*, vol. 50, pp. 293–300, 1999.

[2] M. J. McKeown and R. Radtke, "Phasic and tonic coupling between EEG and EMG demonstrated with independent component analysis," *J. Clin. Neurophysiol.*, vol. 18, no. 1, pp. 45–57, 2001.

[3] A. d'Avella, P. Saltiel, and E. Bizzi, "Combinations of muscle synergies in the construction of a natural motor behavior," *Nat. Neurosci.*, vol. 6, no. 3, pp. 300–308, 2003.

[4] M. J. McKeown, "Cortical activation related to arm-movement combinations," *Muscle Nerve Suppl.*, vol. 9, pp. 19–25, 2000.

[5] M. C. Tresch, V. C. K. Cheung, and A. d'Avella, "Matrix factorization algorithms for the identification of muscle synergies: Evaluation on simulated and experimental data sets," *J. Neurophysiol.*, vol. 95, no. 4, pp. 2199–2212, 2006.

[6] P. Davidson, R. Jones, and J. Andreae *et al.*, "Simulating closed- and open-loop voluntary movement: A nonlinear control-systems approach," *IEEE Trans. Biomed. Eng.*, vol. 49, no. 11, pp. 1242–1252, 2002.

[7] D. Farina and R. Merletti, "Comparison of algorithms for estimation of EMG variables during voluntary isometric contractions," *J. Electromyogr. Kinesiol.*, vol. 10, no. 5, pp. 337–349, 2000.

[8] Z. Ghahramani, "An introduction to hidden Markov models and Bayesian networks," *Int. J. Pattern Recognit. Artif. Intell.*, vol. 15, no. 1, pp. 9–42, 2001.

[9] S. Dey, V. Krishnamurthy, and T. Salmon-Legagneur, "Estimation of Markov-modulated time-series via EM algorithm," *IEEE Signal Process. Lett.*, vol. 1, no. 10, pp. 153–155, 1994.

[10] M. Cassidy and P. Brown, "Hidden Markov based autoregressive analysis of stationary and non-stationary electrophysiological signals for functional coupling studies," *J. Neurosci. Methods*, vol. 116, no. 1, pp. 35–53, 2002.

[11] E. Clancy, E. Morin, and R. Merletti, "Sampling, noise-reduction and amplitude estimation issues in surface electromyography," *J. Electromyogr. Kinesiol.*, vol. 12, no. 1, pp. 1–16, 2002.

[12] X. Hu and V. Nenov, "Multivariate AR modeling of electromyography for the classification of upper arm movements," *Clin. Neurophysiol.*, vol. 115, no. 6, pp. 1276–1287, 2004.

[13] J. Li, Z. J. Wang, J. J. Eng, and M. J. McKeown, "Bayesian network modeling for discovering depedent synergies among muscles in reaching movements," *IEEE Trans. Biomed. Eng.*, vol. 55, no. 1, pp. 298–310, Jan. 2008.

[14] K. P. Murphy, Switching Kalman Filters Dep. Comput. Sci., Univ. Calif., Berkeley, 1998, Tech. Rep..

[15] T. K. Moon, "The expectation-maximization algorithm," *IEEE Signal Process. Mag.*, vol. 13, no. 6, pp. 47–60, 1996.

[16] L. R. Rabiner, "A tutorial on hidden Markov models and selected applications inspeech recognition," *Proc. IEEE*, vol. 77, no. 2, pp. 257–286, 1989.

[17] R. Milo, S. Shen-Orr, and S. Itzkovitz *et al.*, "Network motifs: Simple building blocks of complex networks," *Science*, vol. 298, no. 5594, pp. 824–827, 2002.

[18] R. V. Hogg and J. Ledolter, *Engineering Statistics*. New York: Macmillan, 1987.

[19] L. Brieman, J. H. Friedman, and R. A. Olshen *et al.*, "Classification and regression trees," *Wadsworth Inc.*, vol. 67, 1984.

[20] C. J. Burges, "A tutorial on support vector machines for pattern recognition," *Data Mining and Knowledge Discov.*, vol. 2, no. 2, pp. 121–167, 1998.

[21] J. Chiang, Z. J. Wang, and M. J. McKeown, "Hidden Markov multivariate autoregressive (HMM-mAR)modeling of dynamic muscle association patterns in reaching movements," in *Proc. 29th Can. Med. Biolog. Soc. Conf. (CMBES29)*, 2006.

[22] P. H. McCrea, J. J. Eng, and A. J. Hodgson, "Saturated muscle activation contributes to compensatory reaching strategies after stroke," *J. Neurophysiol.*, vol. 94, no. 5, pp. 2999–3008, 2005.

[23] N. E. Huang, Z. Shen, and S. R. Long *et al.*, "The empirical mode decomposition and the Hilbert spectrum for nonlinear and non-stationary time series analysis," *Proc. Math. Phys. Eng. Sci.*, vol. 454, no. 1971, pp. 903–995, 1998.

[24] M. J. McKeown, R. Saab, and R. Abu-Gharbieh, "Combined independent component analysis (ICA)/empirical mode decomposition (EMD) method to infer corticomuscular coupling," in *Proc. 2nd Int. IEEE EMBS Neural Eng. Conf.* , 2005, pp. 679–682.

[25] H. Lütkepohl, "Comparison of criteria for estimating the order of a vector autoregressive process," *J. Time Series Anal.*, vol. 6, no. 1, pp. 35–52, 1985.

[26] A. d'Avella, A. Portone, and L. Fernandez *et al.*, "Control of fast-reaching movements by muscle synergy combinations," *J. Neurosci.*, vol. 26, no. 30, p. 7791, 2006.

Joyce Chiang received the B.A.Sc. and M.A.Sc. degrees in electrical and computer engineering from the University of British Columbia (UBC), Canada, in 2004 and 2007, respectively.

She is currently pursuing the Ph.D. degree at UBC. Her research interest is in statistical signal processing with applications to biomedical signals.

Z. Jane Wang (M'02) received the B.Sc. degree from Tsinghua University, China, in 1996, with the highest honor, and the M.Sc. and Ph.D. degrees from the University of Connecticut, Storrs, in 2000 and 2002, respectively, all in electrical engineering.

While at the University of Connecticut, she received the Outstanding Engineering Doctoral Student Award. She has been Research Associate of the Institute for Systems Research, University of Maryland, College Park. Since August 1, 2004, she has been with the Department Electrical and Computer Engineering, University of British Columbia (UBC), Canada, as an Assistant Professor. Her research interests are in the broad areas of statistical signal processing, with applications to information security, biomedical imaging, genomic and bioinformatics, and wireless communications. She coedited a book, *Genomic Signal Processing and Statistics*, and coauthored a book, *Multimedia Fingerprinting Forensics for Traitor*.

Dr. Wang was a corecipient of the EURASIP Best Paper Award 2004 and IEEE Signal Processing Society Best Paper Award 2005, and a Junior Early Career Scholar Award from Peter Wall Institute at UBC in 2005. She is an Associate Editor for the *EURASIP Journal on Bioinformatics and Systems Biology*.

Martin J. McKeown received the B.S degree (*summa cum laude*) in engineering physics from McMaster University, Canada, in 1986, and the M.D. degree from the University of Toronto, Canada, in 1990.

From 1990 to 1994, he specialized in neurology at the University of Western Ontario, Canada, and later did a fellowship in clinical electrophysiology. From 1995 to 1998, he was a research associate with the Computational Neurobiology Lab, Salk Institute for Biology Studies, San Diego, CA. During 1998–2003, he was an Assistant Professor of Medicine at Duke University, Durham, NC, core faculty at Dukes Brain Research and Analysis Center, as well as an adjunct professor in Biomedical Engineering and Dukes Center for Neural Analysis. He is currently an Associate Professor of Medicine (Neurology) and faculty member of the Pacific Parkinsons Research Center, and the Brain Research Centre at the University of British Columbia. His current work includes electrophysiology and fMRI as it pertains to patients with movement disorders. In addition to research, he trains physicians in neurology and treats patients with Movement Disorders, such as Parkinsons disease.

Dr. McKeown is Board Certified in neurology in Canada and the U.S., and has been an examiner for the U.S. Neurology Board certification.